

# Lane Detection and Road Surface Reconstruction Based on Multiple Vanishing Point & Symposia\*

BiJun Li, Yuan Guo, Jian Zhou, Yi Cai, JinSheng Xiao and Weicheng Zeng

**Abstract**— Lane detection algorithm based on monocular camera is one of the most popular methods in recent years, which can meet the requirement of real-time and robust for autonomous vehicle. In this way, the position of lane markers can be transferred from perspective space to road space base on the planar road assumption. However, large numbers of road scenes, especially the up and down slope road environment, cannot meet this requirement.

In this paper, we propose a multiple vanishing point detection method to reconstruct the road space in slope scenes. In order to improve the accuracy of vanishing point estimation, the road images are decomposed into near and far regions. We extract candidate lane markers in near region by using multiscale convolution kernel and Hough Transform at first. Then, the lane markers in far region can be detected based on the result of near region. At last, different vanishing points are extracted in near and far regions. With the help of a vanishing point based on camera model, we can project both of near and far regions into road space. The experiment is conducted on our self-driving car ‘TuLian’ in campus environment.

## I. INTRODUCTION

Lane detection plays a key role in autonomous vehicles and Advance Driver Assist System (ADAS). As a basic part of these driving support systems, real-time and robust lane detection algorithms can provide direction and departure information to ensure comfort driving behaviors. There are many kinds of sensors used for lane detection, such as binocular camera [1] and LIDAR [2]. However, monocular camera is one of the most popular solutions in recent years. Lane detection algorithms based on monocular camera have been proposed in the last decades, including the feature-based method and model-based method. Both of them must project the lane marker detection results into road space and provide 3D coordinate. But we cannot calculate 3D coordinate of lane marker in road space from a single monocular image, so most of the works aim to structure road based on a planar road assumption. However, there always exist large numbers of road scenes to solve, for instance, the up or down slope road, bridge, ramp, etc. In these road scenes, extrinsic parameters

between camera and flat segments are different with each other. So, fixed extrinsic camera parameters must be introduced to an incorrect inverse perspective mapping (IPM) [3] which can project lane markers from image space to road space.

In this work, we present a multiple vanishing point based on road scenes reconstruction method to solve the problem mentioned previously. As vanishing point is the unique feature to distinguish different surface segments, the accuracy of vanishing point estimation is very important for the final reconstruction result. A vanishing point detection method called CHEVP (Canny/Hough Estimation of Vanishing Point) is proposed in paper [4]. However, the Canny algorithm and Hough Transform process for the 1920\*1200 image spends too much computation time which cannot meet the real-time requirement. Another real-time vanishing point detection method is described in [5], but this method estimates vanishing point from global image space which cannot provide multiple vanishing point position in slope road scenes. Because the slope road image includes both the horizontal part near the vehicle and the slope parts far away.

Our proposed approach divides the image into near and far regions. With the help of our previous work [6], candidate lane markers can be extracted in near region based on multiscale gradient convolution kernel and Hough Transform. Lane markers in far regions, which are thin and blurred compared to near markers, can also be accurately detected based on the robust result of near region. At last, all these vanishing points are utilized to reconstruct the slope road surface.

The paper is structured as follows. Section II discusses the algorithm of lane detection. And the vanishing point extraction is discussed in section III. The road surface reconstruction method is detailed in section IV. Section V present the experiment of the algorithm above on a self-driving platform. At last, a conclusion is presented in section VI.

## II. LANE DETECTION

Our proposed method is composed of three steps: feature extraction, model estimation and parameters tracking. In this paper, we focus on the first two steps, because the third step has been proposed in our previous work [6] which tracks lane parameters with External Kalman Filter (EKF).

\*Resrach supported by the National Natural Science Foundation (41671441; 41531177; U1764262)

Yuan Guo, Jian Zhou, Yi Cai and Bijun Li are with the State Key Laboratory of Information Engineering in Surveying, Mapping and Remote Sensing, Wuhan University, China; (e-mail: [guoyuan@whu.edu.cn](mailto:guoyuan@whu.edu.cn); [zj2007@whu.edu.cn](mailto:zj2007@whu.edu.cn); [charyee@126.com](mailto:charyee@126.com); [Lee@whu.edu.cn](mailto:Lee@whu.edu.cn)). Jinshen Xiao are with the Electronic Information School, Wuhan University, China; (e-mail: [xiaoj@whu.edu.cn](mailto:xiaoj@whu.edu.cn)) Weicheng Zeng are with the College of Electronic and Information Engineering (CEIE), Tongji University, China; (e-mail: [1006628465@qq.com](mailto:1006628465@qq.com)).

### A. Feature extraction

As the road surface can't keep flat all the time, the paralleled road lanes will intersect each other in a top-view which created by traditional IPM. We decompose the whole image into near and far regions. Because of the perspective transform, road lane in near region is longer and more distinct than far region. So, we extract the edge feature of road lanes in near region at first.

A typical lane marker consists of two symmetrical edges. Gray values between the two edges are brighter than the cement or asphalt background. In order to utilize these two characters, our approach builds a specific convolution kernel for every image row. While the maximal width  $S_m$  and the minimal width  $S_M$  are linear changed along vertical coordinate of image [9], we can calculate the accurate width in all image rows. After initialized edge width of lane marker of all image rows, we design a convolution kernel to calculate gradient. The kernel size is double of the pixels width of a single lane marker in specific image row. The process can be described as in (1).

$$E_j = \begin{cases} 1/L \sum_{k=1}^l I_{j+k} - I_{j-k} & j = j_{min} \\ E_{j-1} + \frac{1}{L} (I_e - I_m) & j \in (j_{min}, j_{max}) \end{cases} \quad (1)$$

where  $E_j$  is gradient value, and  $L$  is the width of the convolution kernel size. To improve efficiency of the algorithm, the convolution kernel initialized when the scan line starts and then update the pixels at the end of the convolution kernel.

As the "Fig. 1" show, the red line means the gray value of pixels along a scanning line. The convolution kernel with specified width, slide from left to right. At last, pairs of points with symmetrical gradient and appropriate pixel width between  $S_{min}$  and  $S_{max}$  are selected for candidate feature points.  $S_{min}$  and  $S_{max}$  are min and max pixel width for specified scanline.

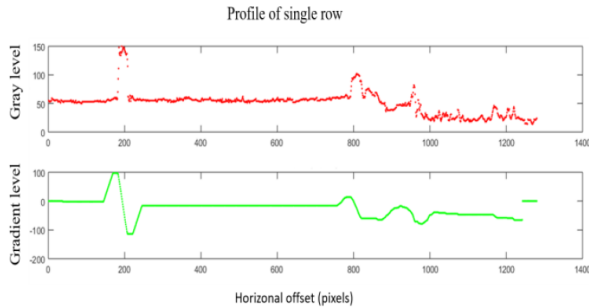


Figure 1. Edge detection process of single rows. Red profile: raw gray level of a specific image row. Green profile: gradient value of specific image row with accurate convolution kernel size.

### B. Near Region Detection

A road lane can also be decomposed of single or multiple straight lane segment [10], although many curve models of

ego-lane have been proposed in the present state of the art. Compared to curve models, straight line models consume little computation and get closed accuracy in some road condition, especially near region from the vehicle [7].

The Hough Transform is applied for line segment extraction in near region. The difference of it is that we transfer the feature points from perspective coordinate of image to road coordinate. All the feature points are projected to a rectangle region near the vehicle with width  $W$  and distance  $D$ , and  $W$  and  $D$  can be set as fixed road parameters.

In order to extract lane segments in near region timely, we use a novel Hough Transform which proposed in our previous work [6]. As we show in "Fig. 2", every line segment can be described as offset  $p$  and yaw angle  $q$ . At first, we create a voting map for near region which is equal to the proportion of region of interest (ROI) in detection region. Then, we transfer all the feature points which are extracted in feature extraction into the voting map with intrinsic and external parameters of camera. At last, the offset parameter  $p$  traversed from left to right in the voting map, and we select line segment which contain maximal voting number and exceed voting threshold at every offset.

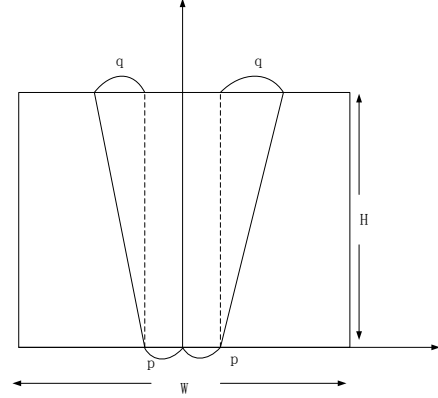


Figure 2. Hough Transform space: every line can be described as a unique offset  $p$  and yaw angle  $q$ .

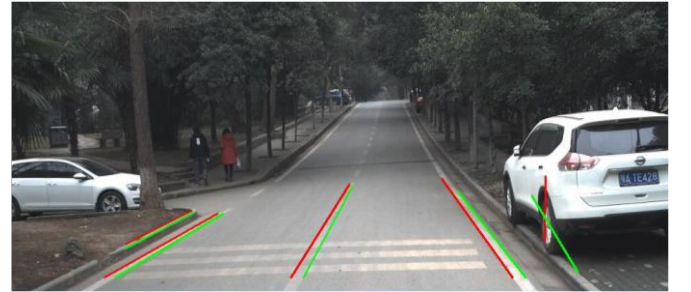


Figure 3. Line segment detection in near region. Red lines: line segments with positive gradient. Green lines: line segments with negative gradient.

According to "Fig. 3", line segments detection by Hough Transform always contain some error results. As a lane segment containing double edges which parallel with each other in road space, we pair the line segments with each other and select edge pairs with same offset and yaw as a candidate of lane feature. Then, the road width and number of points are

used to avoid error detections like trees, guiderails, shadows and other, as “Fig. 4” show.

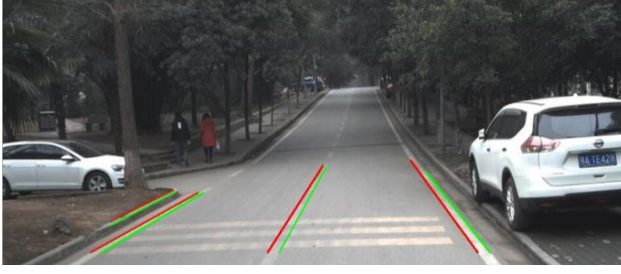


Figure 4. Lane marker in near region

### C. Far Region Detection

Compared to near region, lane detection process in far region is more complex. Because of the perspective transformation, the width of road surface will become narrower along the photogrammetry direction, and line segments detection may influence by trees, light poles and some other rod object along road, just like “Fig. 5” show.



Figure 5. Line segments influenced by trees

As lane segments have been extracted in near region, we can utilize the priori information in near region to enhance the robust of lane detection in far region. After extending lane markers in near region, we can reduce the detection areas and remove some obviously error result as in “Fig. 6”.

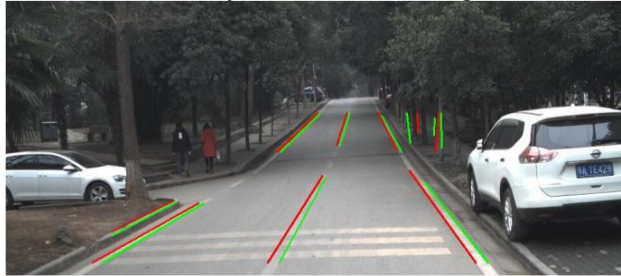


Figure 6. Lane markers in near region and far region

Finally, we need to select the optimal markers for the whole image. The link relation between near region and far region is considered. Since line segments are parameterized with offset  $p$  and yaw angle  $q$  in part B, we extract global lane segment which have similar offset and yaw in near and far region. As show in Fig7, putative outliers are removed after global optimization.

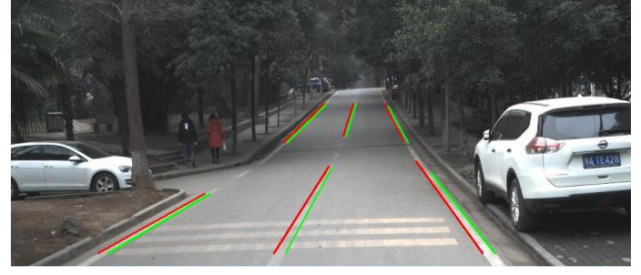


Figure 7. Global optimal result

## III. VANISHING POINTS ESTIMATION

Vanishing points are widely used in unmanned ground vehicles. An accurate position of vanishing point in single monocular image not only can guide the vehicle to correct direction but also will calibrate the external parameters of the camera.

The translation relationship of the coordinate value of lane between the image coordinate system and camera coordinate system can be set up by the geometric model of camera, as show in “Fig. 8”

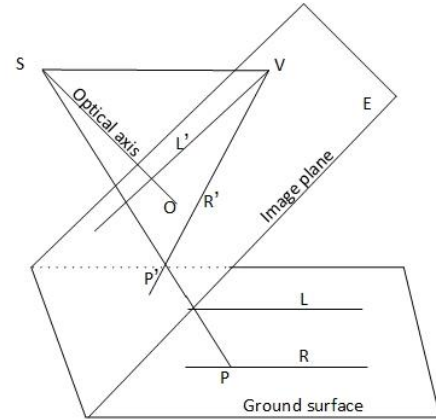


Figure 8. Geometric model of camera.

$L$  and  $R$  are two parallel lanes on the ground and the  $L'$  and  $R'$  are the perspective transformation result of  $L$  and  $R$ . Two parallel lanes in three-dimensional meet at infinity far. However, in the image plane, the two lanes will cross at a point called vanishing point. The vanishing point of  $L$  and  $R$  is  $V$  as show in “Fig. 8”.

The line connecting point  $V$  and the optical center  $S$  have the same direction with the corresponding lines in 3D space that means  $SV$  is parallel to  $L$  and  $R$  [4].

Although many algorithms have been proposed in the literature, most of them always aim to extract accurate coordinate of vanishing point in single image with a global optimal process. However, there always more than one vanishing point in a slope road scene. In section II, we have detected lane markers in slope road scene by divided the whole image into near region and far region. According to paper [11], the accuracy of vanishing point is influenced by length of the lines and angle between them. In order to ensure



the robust and accurate of vanishing point, we use the lane markers to calculate position of vanishing points.

The method we proposed for vanishing point detection include two stages, rough extraction and accurate extraction. In rough extraction stage, vanishing point is used to shrink the range of lane segments, called local estimation. We can exclude some absolutely error line segment by the direction information. This step is used for line segments detection in near region. Then, in accurate extraction stage, we consider near region and far region and select optimal lane markers to calculate vanishing points, called global estimation.

#### A. Local Estimation

After extracted the lane segment in near region, we estimate the location of vanishing points based on the theory that the position accuracy of vanishing point is influenced by the length of line and intersection angle between both lines. Vanishing point with longer length of both lines and the intersection angle closer to  $90^\circ$  can lead to a better evaluate result.

We separate the road model into left and right side, all candidate vanishing points must be estimated from pair of lane marker in different side. On the one hand, with the help of this strategy, lane markers are always longest line segment in near region. On the other hand, different lane side can ensure the intersection angle close enough to  $90^\circ$ . Both of these characters are applied to enhance the position accuracy of vanishing point.

The location of the corresponding vanishing point hypothesis can be computed as in (2).

$$V_{ij} = m_{il} \cdot m_{jr} \quad (2)$$

where  $m_{il}$  and  $m_{jr}$  are homogeneous coordinates of left and right lane segments.

$$W_{ij} = ||V_{ij}|| \cdot l_i \cdot l_j \quad (3)$$

We use the Mahalanobis Distance  $l_i$  and  $l_j$  to define the length of lane marker to magnified length part in weight, as in (3).

#### B. Global Optimization

The whole image are divided to different region from near to far according to the camera. As candidate lane markers have been extracted in previous steps. Lane segments in far region are detected by the help of near region with similar processes. The difference of the linear relationship between edge width and image rows was changed.

As the road surface in far region is a flat surface, we can use the edge width of top row in near region as the bottom edge width of far region. Then, a fixed convolution kernel size is set to extract feature points in far region while edge width reduces gradually from bottom to top.

At last, we classified line segments in different region with the same offset and yaw parameters. For each candidate lane marker in near region with offset  $d_n$  and yaw angle  $y_n$ , if a lane

segment in far region with offset  $d_f$  meet  $d_n + y_n$ , both of them would be classified as one side of ego-lane. As show in “Fig. 9” vanishing point of far region can be calculated with the same method used in near region.

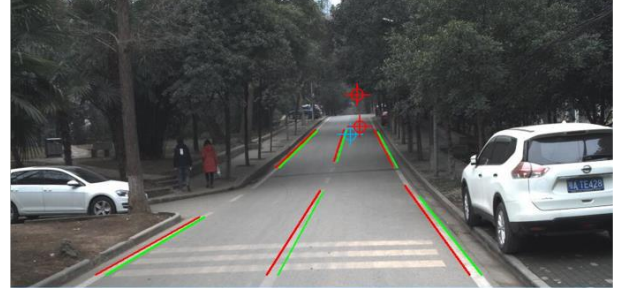


Figure 9. Estimation of vanishing points. Blue mark: local vanishing point estimation. Red mark: global optimization.

### IV. ROAD SURFACE RECONSTRUCTION

Large numbers of lane detection algorithms have been proposed to extract straight, curve, single or multiple lanes in the state of art, and the position of lane marker can be calculated with an inverse perspective mapping(IPM) method which is based on a planar road assumption. However, there are still some road scenes contain slope region which would lead to an error work.

If an up-slope there, the position of vanishing point is above the vanishing point of plane. Conversely, the position of vanishing point will under the vanishing point of plane, when there is a down-slope. As “Fig.10” show. In order to handle these up-slope or down-slope road, we propose a multi-view based on lane detection method.

Furthermore, the distance between the vanishing points is proportional to the slope of the ground, making the result of the lane detection a mistake. As a result, the self-driving car can't get the correct coordinate value of lane marking. To solve the problem, this paper reconstructed the surface of ramp road using multiple vanishing point.

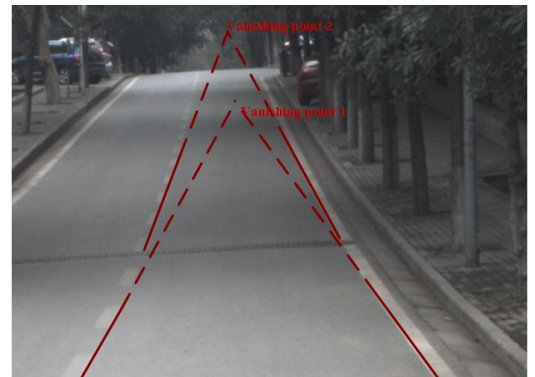
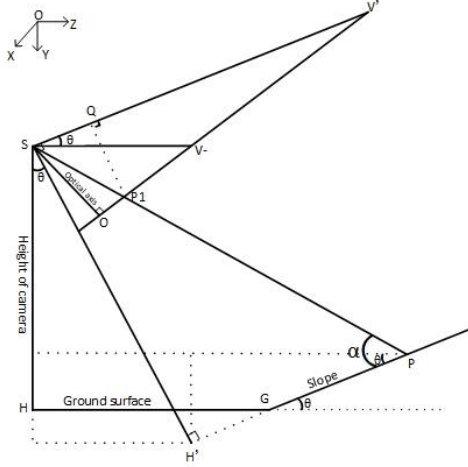
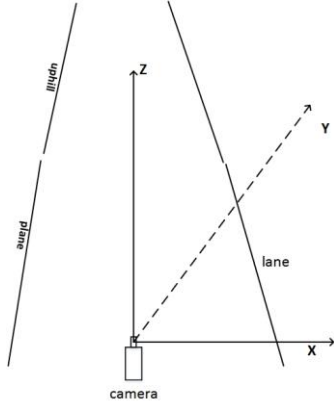


Figure 10. Position of vanishing points.

After the multiple vanishing points detection process, the 3D model of plane and slope are established in this paper, using perspective transformation theory, as displayed in “Fig. 11”.



(a) Top view of the 3D model



(b) Top view of the 3D model

Figure 11. 3D model of slope.

S is the center of projection, so SH is the optical axis of camera. HG and GP represent the plane and slope, respectively. Besides, point V- is the vanishing point of lane in plane and point V' represents the vanishing point of lane in slope. P is any point on the ground.

From the model, the relationship of the coordinate value of lane in plane and slope can be calculated easily. The angle between HG and GP indicated by  $\theta$ , and  $\theta$  can be calculated by the coordinate value of the vanishing points V' and V-, as in (4).  $\alpha$  means the angle between GP and SP, as in (5).  $P_z$ ,  $P_y$  and  $P_x$  are the coordinates of P in camera coordinate system, as in (6)-(8).  $X_p$  and  $Y_p$  are the coordinates of P in image coordinate system.  $k$  is the proportion value of focal length and the coordinate of V' in the image coordinate system.  $f$  means the focal length of camera.

$$\theta = \arctan(V'_y/f) - \arctan(V_-/f) \quad (4)$$

$$\alpha = \arctan(V'_y/f) - \arctan(V_p/f) \quad (5)$$

$$P_z = SH' \cdot \tan \alpha \cdot \cos \theta + SH' \cdot \sin \theta \quad (6)$$

$$P_y = (P_z - SH' / (\tan \alpha \cdot \cos \theta)) / \tan \theta \quad (7)$$

$$P_x = X_p \cdot SH' \cdot k / (V'_y - Y_p) \quad (8)$$

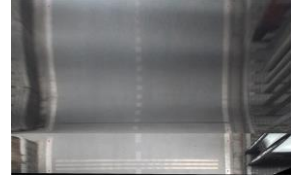
## V. EXPERIMENT

We test the algorithm of this paper on the self-driving car 'Tu Lian', as show in "Fig. 12". The camera we used is POINT GREY BFLY-PGE-23S6C-C.



Figure 12. 'TuLian' self-driving car

We choose an up-slope, down-slope and an on-ramp to test the 3D model. The camera was calibrated first and the focus length is 2246 mm. We compared the method proposed in this paper to the IPM, as in "Fig. 13". After the road reconstruction process, the angle between plane and slope is recovered and the lane keep parallel again, as shown in "Fig. 14". In the up-slope scene, the angle between the plane and slope is  $2.44^\circ$ . The angle of down-slope is  $2.17^\circ$ . And the on-ramp is of  $1.32^\circ$ , which is consistent with actual condition.



(a) proposed result(up)



(b) IPM(up)



(c) proposed result(down)



(d) IPM(down)

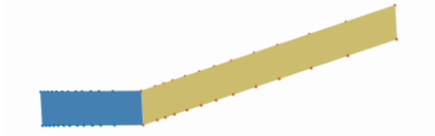


(e) proposed result(on-ramp)



(f) IPM(on-ramp)

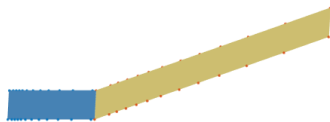
Figure 13. compared to IPM method



(a) The result of up-slope



(b) The result of down-slope



(c) The result of on-ramp

Figure 14. The result of road reconstruction

## VI. CONCLUSION

In this paper, we have proposed an approach for lane detection. To solve the image distortion caused by the slope, the multiple vanishing points are extracted to reconstructed the road surface. Experiments show that the angle between plane and slope is correctly calculated by the model that we proposed in this paper. Meanwhile, the width between the lanes keep consistent after the process. However, the scene of the experiment only estimated two vanishing points in this paper. We collected many road scene, the roads more than two vanishing points are scarce. And we will add this part in our future experiments.

## REFERENCES

- [1] U. Ozgunalp, R. Fan, X. Ai, and N. Dahnoun, "Multiple Lane Detection Algorithm Based on Novel Dense Vanishing Point Estimation," *IEEE Trans. Intell. Transp. Syst.*, vol. 18, no. 3, pp. 621–632, Mar. 2017.
- [2] Q. Li, L. Chen, M. Li, S. L. Shaw, and A. Nuchter, "A Sensor-Fusion Drivable-Region and Lane-Detection System for Autonomous Vehicle Navigation in Challenging Road Scenarios," *IEEE Trans. Veh. Technol.*, vol. 63, no. 2, pp. 540–555, 2014.
- [3] M. Aly, "Real time Detection of Lane Markers in Urban Streets," *ArXiv e-prints*, vol. 1411, p. arXiv:1411.7113, Nov. 2014.
- [4] Y. Wang, E. K. Teoh, and D. Shen, "Lane detection and tracking using B-Snake," *Image and Vision Computing*, vol. 22, no. 4, pp. 269–280, Apr. 2004.
- [5] M. Nieto and L. Salgado, "Real-time robust estimation of vanishing points through nonlinear optimization," 2010, p. 772402.
- [6] P. Hong, J. S. Xiao, C. Xian, L. I. Bi-Jun, and S. Xiao, "Lane detection algorithm based on extended Kalman filter," *Journal of Optoelectronics · Laser*, vol. 26, no. 3, pp. 567–574, 2015.
- [7] L. Chen, L. I. Qing-Quan, and Q. Z. Mao, "Lane Detection and Following Algorithm Based on Imaging Model," *China Journal of Highway & Transport*, vol. 24, no. 6, pp. 96–102, 2011.
- [8] Y. Liu, Y. Wu, M. Wu, and X. Hu, "Planar vanishing points based camera calibration," in *Multi-Agent Security and Survivability, 2004 IEEE First Symposium on*, 2004, pp. 460–463.
- [9] T. Veit, J. P. Tarel, P. Nicolle, and P. Charbonnier, "Evaluation of Road Marking Feature Extraction," in *International IEEE Conference on Intelligent Transportation Systems*, 2008, pp. 174–181.
- [10] M. Revilloud, D. Gruyer, and M. Rahal, "A new multi-agent approach for lane detection and tracking," in *IEEE International Conference on Robotics and Automation*, 2016, pp. 3147–3153.
- [11] B. Lee, J. Zhou, M. Ye, and Y. Guo, "A Novel Approach to Camera Calibration Method for Smart Phones Under Road Environment," *ISPRS - International Archives of the Photogrammetry, Remote Sensing and Spatial Information Sciences*, vol. XLI-B5, pp. 49–54, 2016.